J Pharmacol Sci **117**, 189 – 203 (2011)

Journal of Pharmacological Sciences

Full Paper

Protection Against Dopaminergic Neurodegeneration in Parkinson's Disease–Model Animals by a Modulator of the Oxidized Form of DJ-1, a Wild-type of Familial Parkinson's Disease–Linked PARK7

Masatoshi Inden[1,#], Yoshihisa Kitamura[1,*a], Kazunori Takahashi[2], Kazuyuki Takata[1], Natsuko Ito[1], Rina Niwa[1], Risa Funayama[1], Kaneyasu Nishimura[1], Takashi Taniguchi[1], Toshio Honda[2], Takahiro Taira[3], and Hiroyoshi Ariga[4,*b]

[1]*Department of Neurobiology, Kyoto Pharmaceutical University, Kyoto 607-8414, Japan*
[2]*Faculty of Pharmaceutical Sciences, Hoshi University, Tokyo 142-8501, Japan*
[3]*Department of Molecular Cell Biology, Interdisciplinary Graduate School of Medicine and Engineering, University of Yamanashi, Chuo 409-3898, Japan*
[4]*Department of Molecular Biology, Graduate School of Pharmaceutical Sciences, Hokkaido University, Sapporo 060-0812, Japan*

Received August 19, 2011; Accepted September 29, 2011

Abstract. DJ-1, Parkinson's disease PARK7, acts as an oxidative stress sensor in neural cells. Recently, we identified the DJ-1 modulator UCP0054278 by *in silico* virtual screening. However, the effect of the peripheral administration of UCP0054278 on an in vivo Parkinson's disease (PD) model is unclear. Therefore, in the present study, we examined the effects of the peripheral administration of UCP0054278 on both 6-OHDA–microinjected rats and rotenone-treated mice as acute and chronic animal models of PD, respectively. The peripheral administration of UCP0054278 prevented 6-OHDA– and rotenone-induced dopaminergic neural cell death and restored the defect in locomotion in these models of PD. In addition, 6-OHDA– or rotenone-induced neural cell death and the production of reactive oxygen species were significantly inhibited by UCP0054278 in normal SH-SY5Y cells, but not in DJ-1–knockdown cells. These results suggest that UCP0054278 interacts with endogenous DJ-1 and then produces antioxidant and neuroprotective responses in both in vivo and in vitro models of PD. The present study raises the possibility that DJ-1 stimulatory modulators, such as UCP0054278, may be a new type of dopaminergic neuroprotective drug for the treatment of PD.

Keywords: Parkinson's disease, DJ-1, 6-hydroxydopamine, rotenone, neuroprotection

Introduction

Parkinson's disease (PD) is an age-related neurodegenerative disease that is characterized by relatively selective nigrostriatal dopamine (DA) neurodegeneration and the presence of intraneuronal cytoplasmic inclusions known as Lewy bodies, which are consistently immunostained with antibody to α-synuclein (1, 2). Although the pathophysiological mechanisms of the selective loss of DA neurons are still unclear, it has been suggested that reduced activity of complex I of the mitochondrial respiratory chain in the substantia nigra may be involved in the pathophysiology of PD (3 – 6). In addition, oxidative stress, mitochondrial injury, dysfunction of the ubiquitin-proteasome, and autophagy are thought to trigger the onset of PD. Although genes that have been identified to be responsible for rare familial early-onset PD are thought to play roles in these processes in PD (7 – 13), the precise mechanisms that underlie the onset of PD have not yet been clarified.

DJ-1 was first discovered as a novel oncogene product

[#]Present address: Clinical Pharmacology Laboratory, College of Pharmaceutical Sciences, Ritsumeikan University, Kusatsu 525-8577, Japan
*Corresponding authors.
*[a]yo-kita@mb.kyoto-phu.ac.jp, *[b]hiro@pharm.hokudai.ac.jp
Published online in J-STAGE on October 29, 2011 (in advance)
doi: 10.1254/jphs.11151FP

(14) and was later identified as a causative gene of PD, PARK7 (10). DJ-1 has multiple functions and plays a role in anti-oxidative stress and transcriptional regulation (15 – 29). Although gene mutations in DJ-1 cause loss-of-function, the wild-type DJ-1 plays a key role in anti-oxidation and neuroprotection in neuronal cells (18, 30 – 35). Wild-type DJ-1 in humans and rats has three cysteine residues at amino acid numbers 46, 53, and 106 (C46, C53, and C106, respectively) (36). A cysteine residue is oxidized from a reduced form (-SH) to undergo sulphenation (-SOH), sulphination (-SO_2H), and sulphonation (-SO_3H), in order of oxidative development. Among these three cysteine residues, C106 is the most sensitive to oxidative stress (36). Recently, we used the X-ray crystal structure of DJ-1 oxidized at C106 with the SO_2H form and the three-dimensional coordinate data of about 30,000 chemical compounds in the University Compound Project (UCP) at the Foundation for Education of Science and Technology and performed virtual screening (*in silico*) to search for modulators of DJ-1 binding. Among the DJ-1 modulators identified *in silico*, 2-[3-(benzyloxy)-4-methoxyphenyl]-*N*-[2-(7-methoxy-1,3-benzodioxol-5-yl)ethyl]acetamide (UCP0054278) had the highest binding constant (docking score) toward the pocket of the SO_2H-oxidized C106 region (32). Intranigral co-injection of UCP0054278 with 6-hydroxydopamine (6-OHDA) prevented 6-OHDA–induced dopaminergic neural cell death and restored the defect in locomotion in the rat model of PD. In addition, the intrastriatal pre-injection of UCP0054278 inhibited neurodegeneration induced by occlusion of the middle cerebral artery (MCAO) and reperfusion in rats (34). However, the effect of the peripheral administration of UCP0054278 on an in vivo PD model is unclear.

Unilateral injection of 6-OHDA into the substantia nigra leads to rapid cell death (within 1 – 3 days) (2). Although 6-OHDA has been shown to be useful in the pharmacological screening of drugs, 6-OHDA lesions do not result in the formation of Lewy bodies in the substantia nigra. In addition, the blood–brain barrier (BBB) is damaged by the intranigral injection of 6-OHDA, although the operative procedure is easy. However, a major advantage of the 6-OHDA model is that it gives a quantifiable motor deficit (rotation) (37). On the other hand, we reported that chronic oral administration of rotenone caused specific nigrostriatal DA neurodegeneration in C57BL/6 mice (38, 39). In rotenone-treated mice, α-synuclein immunoreactivity was increased in some surviving tyrosine hydroxylase (TH)-positive neurons in the substantia nigra. The number of α-synuclein and TH double-positive neurons increased in a time-dependent manner. The previous experimental condition in the rotenone model may resemble early PD symptoms rather than atypical parkinsonism, although long-term treatment with rotenone is necessary (38, 39). Therefore, in the present study, we used 6-OHDA–microinjected rats and rotenone-treated mice as acute and chronic animal models of PD, respectively. Briefly, we examined the neuroprotective effect of the peripheral administration of UCP0054278 on 6-OHDA–induced dopaminergic neural cell death in an in vivo model of PD. We also investigated the neuroprotective effect of the peripheral administration of UCP0054278 under the chronic oral administration of rotenone as another in vivo model of PD. Moreover, we determined the neuroprotective effects of UCP0054278 toward 6-OHDA– or rotenone-mediated cell death in normal and DJ-1–knockdown SH-SY5Y cells as an in vitro model of PD.

Materials and Methods

Design of animal experiments

Male Wistar rats (250 g) and male C57BL/6N mice (20 – 25 g) were purchased from Japan SLC, Inc. (Hamamatsu). Animals were acclimated to and maintained at 23°C under a 12-h light/dark cycle (light on 08:00 – 20:00) and housed in standard laboratory cages with free access to food and water throughout the study period. All animal experiments were carried out in accordance with the National Institutes of Health Guide for the Care and Use of Laboratory Animals, and the protocols were approved by the Committee for Animal Research at Kyoto Pharmaceutical University.

At the beginning of the experiment with the hemiparkinsonian rat model (Fig. 1A), rats were devided into four subgroups containing equal numbers of animals: vehicle, pre-treatment, post-treatment, and pre + post-treatment. All rats received a unilateral intranigral injection of 6-OHDA, in order to lesion the nigrostriatal pathway, on the left side in the substantia nigra. In addition, these rats were intraperitoneally injected with either vehicle (1% DMSO) or UCP0054278 at a dose of 1 mg/kg (including 1% DMSO) at 24 h and 30 min before microinjection (pre-treatment), at 24, 48, and 72 h after microinjection (post-treatment), or at 24 h and 30 min before and 24, 48, and 72 h after microinjection (pre + post-treatment) (Fig. 1A). Seven days later, methamphetamine-induced rotation tests were performed. Finally, after the behavior test, rats were sacrificed and the brains were quickly removed for immunohistochemical analysis.

In the second part of this study (Fig. 1B), using rotenone-lesioned mice, we examined the effect of the peripheral administration of UCP0054278 on dopaminergic neurons. UCP0054278 (including 1% DMSO) at a dose of 1 or 3 mg/kg was intraperitoneally injected daily at 30

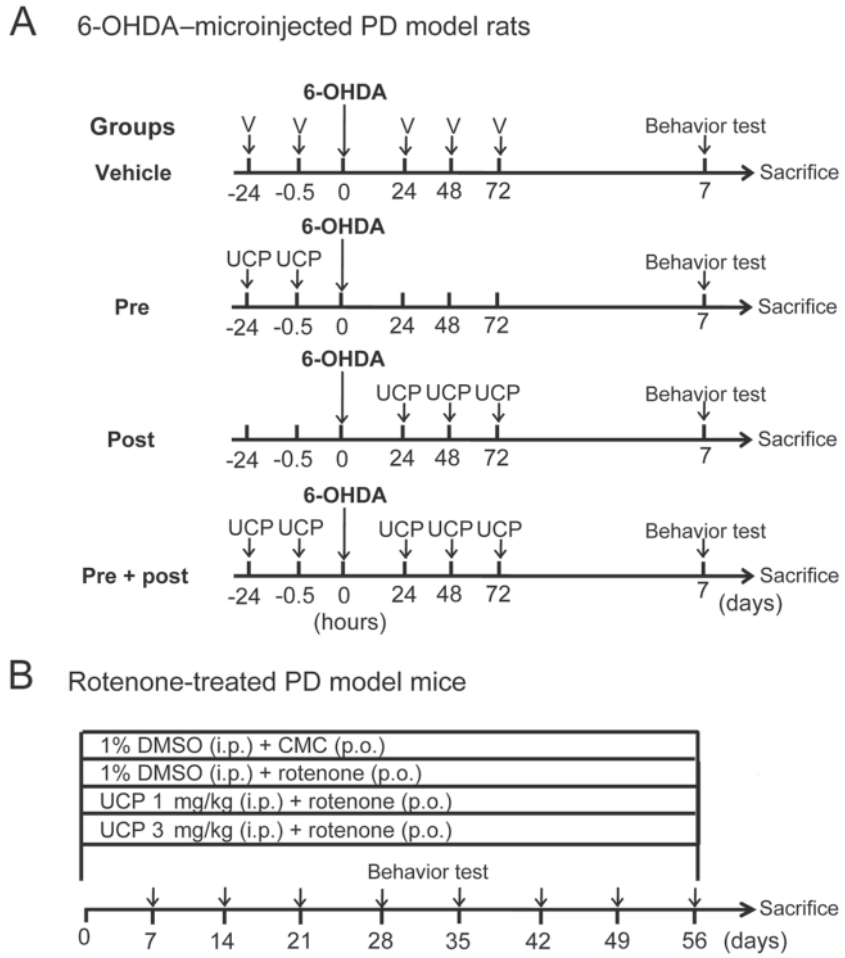

Fig. 1. Experimental design. A: 6-OHDA–microinjected PD model rats. Rats received a unilateral intranigral injection of 6-OHDA on the left side in the substantia nigra and were then devided into four subgroups containing equal numbers of animals: vehicle-group, pre-group, post-group, and pre + post-group. Rats were intraperitoneally injected with either vehicle (1% DMSO, vehicle-group) or UCP0054278 at a dose of 1 mg/kg (including 1% DMSO) at 24 h and 30 min before microinjection (pre-group), at 24, 48 and 72 h after microinjection (post-group), or at 24 h and 30 min before and 24, 48, and 72 h after microinjection (pre + post-group). Seven days later, methamphetamine-induced rotation tests were performed. B: Rotenone-treated PD model mice. UCP0054278 (including 1% DMSO) at a dose of 1 or 3 mg/kg was intraperitoneally injected daily at 30 min before each oral administration of rotenone. Vehicle (1% DMSO) was injected in parallel as a corresponding control. The behavior of each mouse was assessed by the rota-rod test. Finally, after the behavior test, animals were sacrificed and the brains were quickly removed for immunohistochemical analysis. V: vehicle (1% DMSO), UCP: UCP0054278.

min before each oral administration of rotenone. Vehicle (1% DMSO) was injected in parallel as a corresponding control. The behavior of each mouse was assessed weekly by the rota-rod test. Finally, after the behavior tests, mice were sacrificed and the brains were quickly removed for immunohistochemical analysis.

6-OHDA–microinjected PD model rats

For stereotaxic microinjection, rats were anesthetized (sodium pentobarbital, 50 mg/kg, i.p.) and immobilized in a Kopf stereotaxic frame (30). Subsequently, rats were microinjected with 6-OHDA (6 μg, final concentration of 6 mM; Sigma, St. Louis, MO, USA) in a final volume of 4 μL of phosphate-buffered saline (PBS) containing 0.02% ascorbic acid (1.1 mM, as a 6-OHDA stabilizer). The intranigral injection coordinates (4.8-mm anterior-posterior, 1.8-mm left lateral, 7.8-mm ventral from the bregma) were taken from a rat brain atlas. Microinjections were administered by a motor-driven 10-μL Hamilton syringe using a 26-gauge needle. The infusion rate was 1 μL/min, and the injection cannula was kept in place for an additional 5 min after injection.

Assay of drug-induced rotation behavior

We used methamphetamine (Dainippon Pharmaceutical Co., Ltd., Osaka), as a DA-releaser. Drug-induced rotational asymmetry was assessed in rotometer bowls, as described previously (30). Briefly, the numbers of full-body-turn rotations in the ipsilateral direction was counted after the administration of methamphetamine (2.5 mg/kg, i.p., for 70 min).

Rotenone-treated PD model mice

Rotenone (Sigma) was administered orally once daily at a dose of 30 mg/kg for 56 days, as described previously (38, 39). Rotenone was suspended in 0.5% carboxymethyl cellulose sodium salt (CMC; Nacalai Tesque, Kyoto) and administered orally once daily at a volume of 5 mL/kg body weight. CMC (0.5%) was administered orally as vehicle to control mice.

Rota-rod test

The behavior of each mouse was assessed by the rota-rod test, as described previously (38, 39). The rota-rod treadmill (accelerating model 7750; Ugo Basile, Varese,

Italy) consists of a plastic rod, 6 cm in diameter and 36-cm-long, with a non-slippery surface 20-cm above the base (trip plate). This rod is divided into four equal sections by five discs (25 cm in diameter), which enables four mice to walk on the rod at the same time. In the present study, the accelerating rotor mode was used (10-grade speeds from 2 to 20 r.p.m. for 5 min). The performance time was recorded while mice were running on the rod.

Primary antibodies

Primary antibodies included rabbit polyclonal antibodies against TH (Chemicon Int., Temecula, CA, USA), cluster of differentiation antigen-11b (CD11b; Harlan Sera-Lab., Loughbrough, UK), and glial fibrillary acidic protein (GFAP, Chemicon Int.). Mouse monoclonal antibodies against TH (Sigma) and α-synuclein (Transduction Lab., Lexington, KY, USA) were used.

Tissue preparation and immunohistochemistry

After the behavior tests, treated animals were perfused through the aorta with 150 mL of 10 mM PBS, followed by 300 mL of a cold fixative consisting of 4% paraformaldehyde, 0.35% glutaraldehyde, and 0.2% picric acid in 100 mM phosphate buffer (PB), under deep anesthesia with pentobarbital (100 mg/kg, i.p.). After perfusion, the brain was quickly removed and postfixed for 2 days with paraformaldehyde in 100 mM PB and then transferred to 15% sucrose solution in 100 mM PB containing 0.1% sodium azide at 4°C. The brain slices were cut using a cryostat and collected in 100 mM PBS containing 0.3% Triton X-100 (PBS-T). Brain slices were incubated with primary antibody to TH (diluted 1:10,000), GFAP (1:3,000), or CD11b (1:1,000) for 3 days at 4°C. After several washes, slices were incubated with biotinylated anti-mouse or anti-rabbit IgG antibody (1:2,000), as appropriate, for 2 h at room temperature. The slices were then incubated with avidin peroxidase (1:4,000; ABC Elite Kit; Vector Laboratories, Burlingame, CA, USA) for 1 h at room temperature. All of the slices were washed several times with PBS-T between each incubation, and labeling was then revealed by 3,3′-diaminobenzidine (DAB) with nickel ammonium, which yielded a dark blue color.

Measurement of immunoreactive neurons and areas

TH-positive neurons in the substantia nigra pars compacta (SNpc) were estimated using Stereo Investigator software (MBF Bioscience, Williston, VT, USA), and stereologic principles (39). Six sections (60-μm-thick), each separated by 240 μm from the anterior to the posterior midbrain, were used for counting in each case. A BX51 (Olympus, Tokyo) was coupled to an Optronics Microfire digital camera CX9000 (MBF Bioscience) for the visualization of tissue sections. The total number of TH-positive neurons was estimated from coded slides using the optical fractionator method. For each tissue section analyzed, the section thickness was assessed empirically and 5-μm-thick guard zones were used at the top and bottom of each section. The SNpc was outlined under low magnification (× 4) and 10 sites in the outlined region were analyzed using a systematic random sampling design with a grid size of 180 × 180 μm (including the frame size) and a dissector height of 20 μm. Neurons were counted under × 40 magnification. The coefficients of error (CE) were calculated according to the procedure described by the manufacturer, and values < 0.10 were accepted.

The optimal density of TH-fiber in the striatum region was determined using a camera (Progres 3008; Carl Zeiss, Jena, Germany) and a computerized image-analysis system (WinRoof; Mitani, Fukui) (38, 39). The striatal section (20-μm-thick) at 0.48-mm anterior from the bregma was selected and the optimal density was measured within a fixed box (area = 2 × 2 mm) positioned approximately in the middle of the striatal areas.

Double-immunofluorescence staining

For double-immunofluorescence staining, nigral sections of treated mice were incubated with rabbit polyclonal anti-TH antibody (1:5,000; Chemicon Int.) and mouse monoclonal anti-α-synuclein antibody (1:500, Transduction Lab.). The primary antibodies were detected by rhodamine-labeled anti-rabbit IgG (1:500) antibody and fluorescein isothiocyanate (FITC)-labeled anti-mouse IgG antibody (1:500), and fluorescence was observed using a laser scanning confocal microscope (LSM510, Carl Zeiss). Semi-quantitative image-analysis of immunopositive cells was performed on an area of the SNpc.

Cell culture and reactive oxygen species (ROS) production

Using human neuroblastoma SH-SY5Y cells, we established a DJ-1–knockdown cell line (31). Normal and DJ-1–knockdown SH-SY5Y cells were treated with various concentrations of 6-OHDA (25, 50, 75 μM) in the presence of vehicle (0.01% DMSO) or UCP0054278 (containing 0.01% DMSO) for 2.5 h (ROS production) or 24 h (cell survival). In addition, normal and DJ-1–knockdown SH-SY5Y cells were treated with various concentrations of rotenone (100, 300 nM) in the presence of vehicle (0.01% DMSO) or UCP0054278 (containing 0.01% DMSO) for 24 h (ROS production) or 48 h (cell survival). To detect 6-OHDA– or rotenone-induced intracellular ROS production, we used a redox-sensitive

dye, 5-(and-6)-chloromethyl-2′,7′-dichlorodihydrofluorescein diacetate acetyl ester (CM-H_2DCFDA; Invitrogen, Carlsbad, CA, USA), and scanned the fluorescence intensity of oxidized DCF under a confocal microscope (LSM510 META, Carl Zeiss). Cellular images were obtained by difference interference contrast (DIC). Subsequently, we assessed cell viability using 3-(4,5-dimethyl-2-thiazolyl)-2,5-diphenyltetrazolium bromide (MTT; Dojindo Laboratories, Kumamoto).

Statistical evaluation

Results are presented as the mean ± standard error of the mean (S.E.M). The significance of differences was determined by an analysis of variance (ANOVA). Further *post hoc* comparisons were performed using Bonferroni/Dunn tests (Stat View; Abacus Concepts, Berkeley, CA, USA). Endurance performance (percentage of mice remaining on the rota-rod) was calculated by the Kaplan-Meier method. The statistical significance of differences was analyzed by the log-rank (Mantel-Cox) test.

Results

Effect of peripheral administration of UCP0054278 on 6-OHDA–induced movement impairment and dopaminergic neural cell death in hemiparkinsonian rats

To examine the effect of the peripheral administration of UCP0054278 on 6-OHDA–induced dopaminergic neural cell death, UCP0054278 at a dose of 1 mg/kg was intraperitoneally injected at pre-treatment, post-treatment, or pre- and post-treatment (see Materials and Methods "*Design of animal experiments*" and Fig. 1A). Preliminarily, when we intraperitoneally injected the animals with UCP0054278 at a dose of 3 mg/kg, the compound did not cause either neurotoxicity or weight change (data not shown). Thus, toxicity was not observed with UCP0054278 at the concentration used in the present study.

Stereotaxic microinjection of 6-OHDA into the unilateral (left, ipsilateral site) mesencephalon caused behavioral dysfunction (Fig. 2) and a massive loss of TH-positive neurons in the ipsilateral SNpc (Fig. 3). Stimulation with methamphetamine, in rats that had been lesioned unilaterally with 6-OHDA, induced movement ipsilateral to the injection site at 7 days after microinjection (Fig. 2: A and B). Either pre-treatment or post-treatment of UCP0054278 tended to decrease the number of methamphetamine-induced rotations in comparison to non-treated rats, but this difference was not significant. On the other hand, pre- and post-treatment with UCP0054278 significantly ameliorated the methamphetamine-induced behavioral impairment (Fig. 2).

As shown in representative photomicrographs (Fig. 3), TH-positive neurons were obviously preserved under

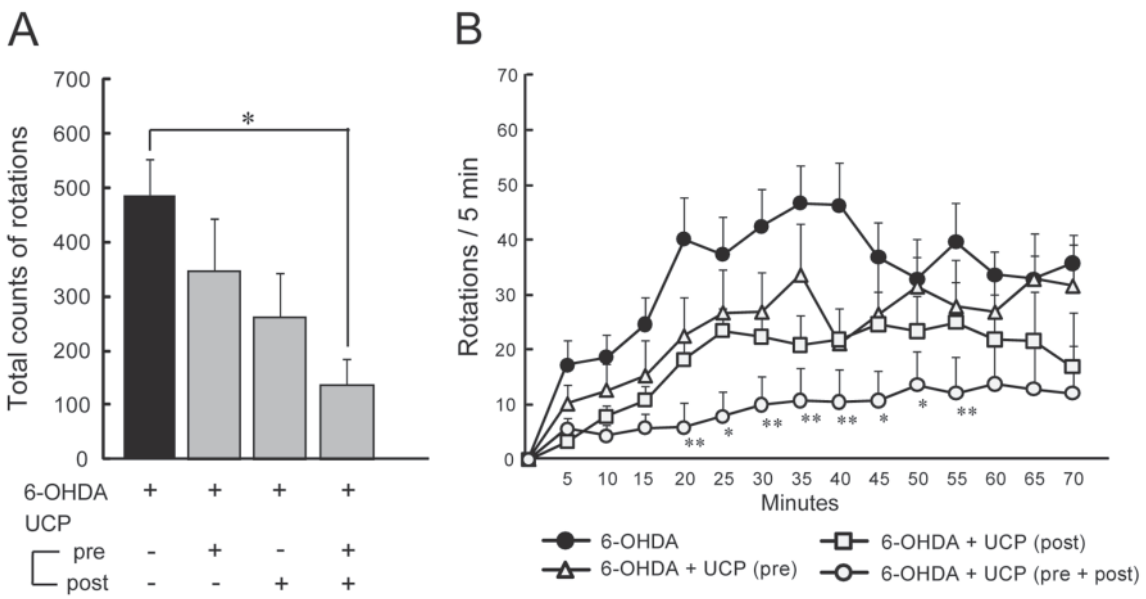

Fig. 2. Effect of UCP0054278 on methamphetamine-induced rotation behavior in rats with intranigral 6-OHDA lesion. A: 6-OHDA–microinjected rats were intraperitoneally injected with either vehicle (1% DMSO) or UCP0054278 at a dose of 1 mg/kg (including 1% DMSO) at 24 h and 30 min before microinjection (pre-treatment), at 24, 48 and 72 h after microinjection (post-treatment), or pre + post-treatment. Seven days later, methamphetamine-induced rotation tests were performed. B: Time-course of rotational behavior. Each value is the mean ± S.E.M. (n = 6 in each group). Significance: *$P < 0.05$, **$P < 0.01$ vs. 6-OHDA alone.

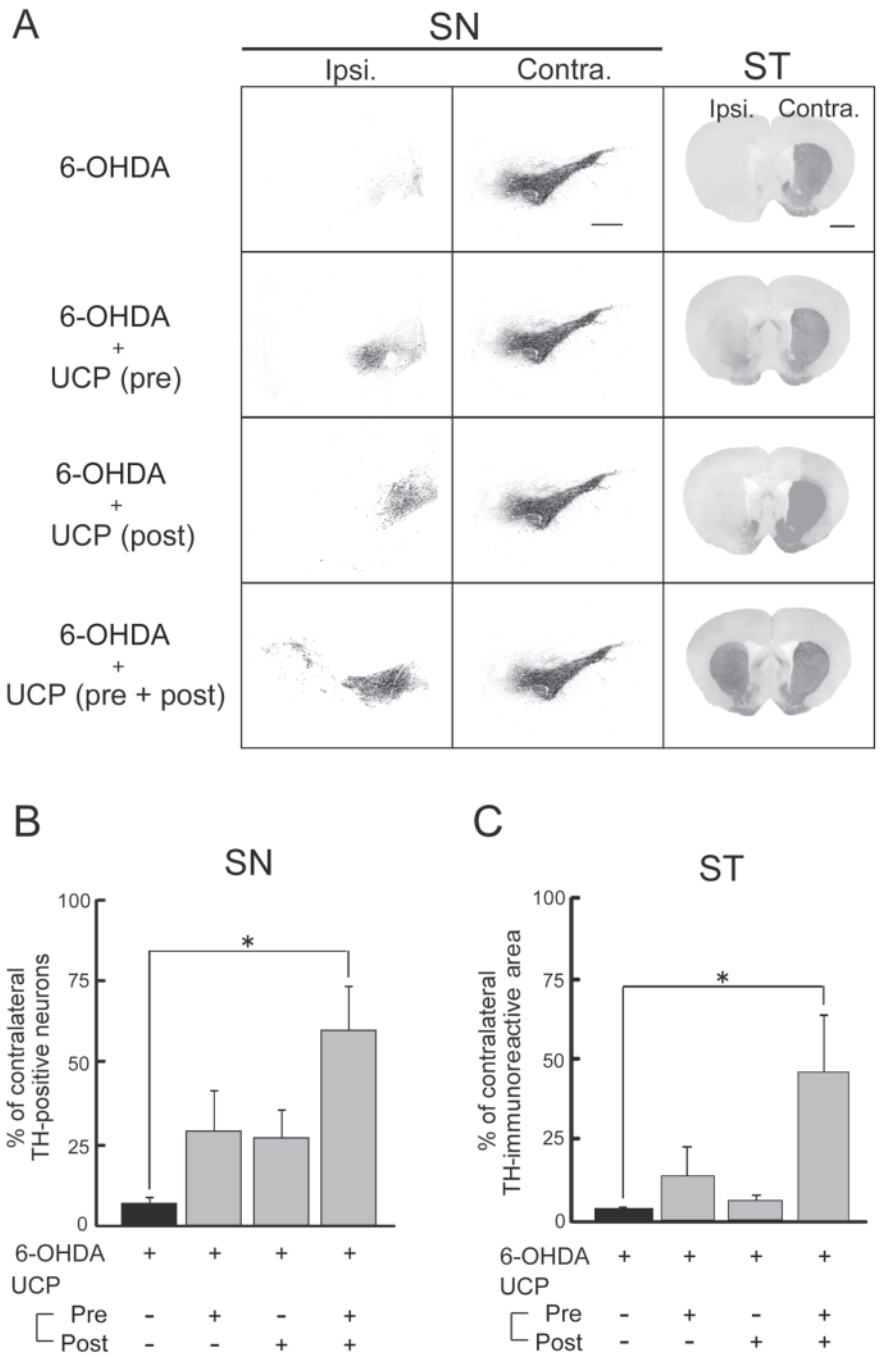

Fig. 3. UCP0054278 prevents the 6-OHDA–induced loss of dopaminergic neurodegeneration. 6-OHDA–microinjected rats were intraperitoneally injected with either vehicle (1% DMSO) or UCP0054278 at a dose of 1 mg/kg (including 1% DMSO) at 24 h and 30 min before microinjection (pre-treatment), at 24, 48, and 72 h after microinjection (post-treatment), or pre + post-treatment. After the behavior test, rats were sacrificed and the brains were quickly removed for immunohistochemical analysis. A: Representative photomicrographs of immunoreactivity for TH in the striatum and substantia nigra. Scale bar: 500 μm. B: Stereological analysis of TH-positive neurons in the substantia nigra. C: Semi-quantitative analysis of TH-immunoreactive areas (mm^2) of the striatum. Each value is the mean ± S.E.M. (n = 6 in each group). Significance: $^*P < 0.05$ vs. 6-OHDA alone.

pre- and post-treatment with UCP0054278 in comparison to non-treated rats at 7 days post-lesion. Stereological analysis of nigral TH-positive neurons showed that the microinjection of 6-OHDA caused a significant loss of DA neurons (Fig. 3B). In contrast, this loss of DA neurons was significantly inhibited by both pre- and post-treatment with UCP0054278. However, this loss of DA neurons was not inhibited by either pre-treatment or post-treatment with UCP0054278 alone.

In the contralateral striatum (non-lesion site), TH immunoreactivity was distinctly detected in dopaminergic fibers (Fig. 3). In the ipsilateral striatum (lesion site), TH immunoreactivity almost completely disappeared in rats that were microinjected with 6-OHDA (Fig. 3A). TH immunoreactivity was slightly detected in 6-OHDA–lesioned rats with either pre- or post-treatment with UCP0054278 alone. However, TH immunoreactivity was significantly restored by both pre- and post-treatment with UCP0054278 (Fig. 3A). Semi-quantitative analysis showed that the intensity of TH-immunoreactivity in the

striatum was significantly increased by both pre- and post-treatment with UCP0054278 compared to the intensity without treatment by UCP0054278 (Fig. 3C).

Effects of peripheral administration of UCP0054278 on glial activation in hemiparkinsonian rats

6-OHDA has been suggested to induce nigrostriatal dopaminergic lesions mediated through the generation of ROS. On the other hand, glial cell activation in response to cellular damage, such as oxidative injury, involves a complex range of responses, including an increase in the expression of several cytokine genes (40, 41). To investigate the effects of UCP0054278 on glial cell activation in 6-OHDA–lesioned rats, we examined immunoreactivities for CD11b and GFAP in the SNpc of 6-OHDA–injected rats under treatment with UCP0054278. In the contralateral SNpc of vehicle-treated rats, immunoreactivities for CD11b and GFAP were detected in the resting forms of microglia and astrocytes, respectively, which had small cell bodies with highly branched and thinner processes (Fig. 4). In response to 6-OHDA lesion, both microglia and astrocytes changed to activated forms that had swollen cell bodies with thicker processes (Fig. 4). The 6-OHDA–induced activation of glial cells was prevented by both pre- and post-treatment with UCP0054278. In addition, pre- or post-treatment with UCP0054278 slightly prevented this glial cell activation (Fig. 4).

Effect of peripheral administration of UCP0054278 on rotenone-induced movement impairment and dopaminergic neural cell death in rotenone-treated mice

Previously, we showed that chronic oral administration of rotenone at 30 mg/kg for 56 days selectively induced nigrostriatal DA neurodegeneration and motor deficits, and increased the cytoplasmic accumulation of α-synuclein in surviving DA neurons (39). To investigate whether UCP0054278 protects DA neurons from damage caused by the chronic oral administration of rotenone (30 mg/kg, i.p. once a day for 56 days), we treated mice with UCP0054278 (1, 3 mg/kg, i.p. once a day for 56 days) 30 min before the oral administration of rotenone (see Materials and Methods "*Design of animal experiments*" and Fig. 1B).

To identify deficits in motor coordination, rotenone-

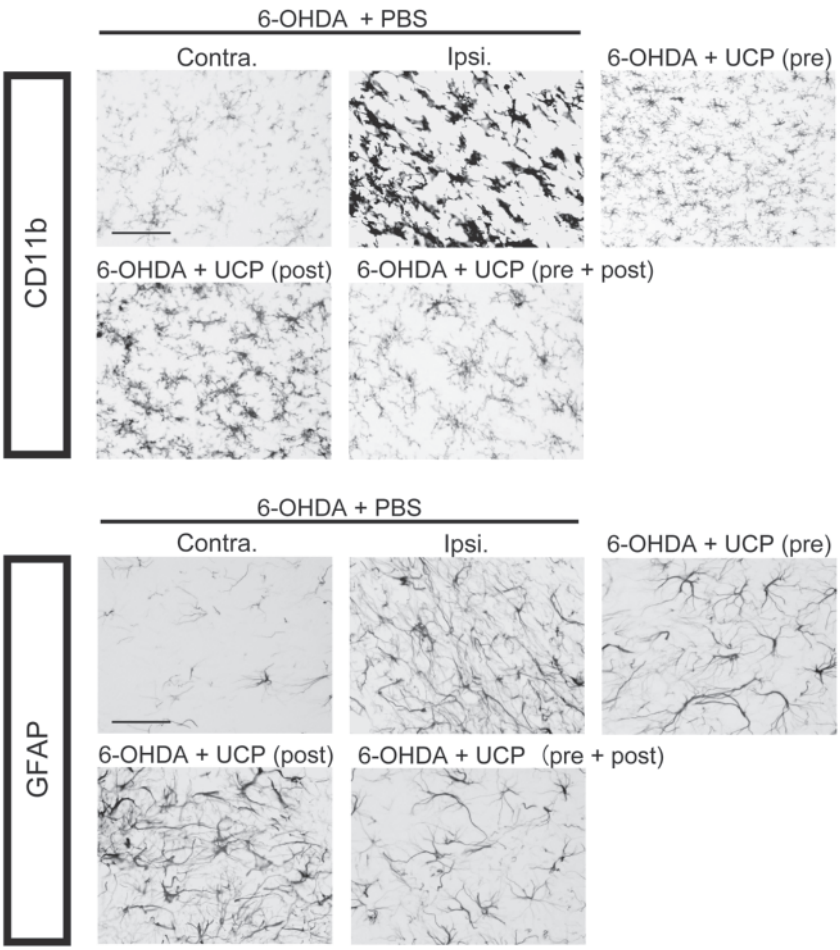

Fig. 4. Representative photomicrographs of immunoreactivities for CD11b (A) and GFAP (B) in the ipsilateral substantia nigra. 6-OHDA–microinjected rats were intraperitoneally injected with either vehicle (1% DMSO) or UCP0054278 at a dose of 1 mg/kg (including 1% DMSO) at 24 h and 30 min before microinjection (pre-treatment), at 24, 48, and 72 h after microinjection (post-treatment), or pre + post-treatment. After the behavior test, rats were sacrificed and the brains were quickly removed for immunohistochemical analysis. Midbrain slices were then immunostained by antibodies against CD11b and GFAP. Scale bar, 60 μm.

treated mice were tested weekly on the accelerating rota-rod. In this condition, vehicle-treated control mice usually remained on the rota-rod for over 300 s under stepwise acceleration. Rotenone-treated mice showed marked reductions in endurance time and in the percentage of mice remaining on the rota-rod. On the other hand, UCP0054278 at both 1 and 3 mg/kg provided a significant functional recovery of the retention time on the rota-rod (Fig. 5).

As shown in representative photomicrographs (Fig. 6), the oral administration of rotenone at 30 mg/kg for 56 days obviously reduced the number of TH-positive neurons in the SNpc (Fig. 6A). Stereological analysis of nigral TH-positive neurons showed that rotenone caused a significant loss of DA neurons (Fig. 6B). To investigate whether UCP0054278 protects DA neurons from damage caused by the chronic oral administration of rotenone, we treated animals with UCP0054278 at either 1 or 3 mg/kg 30 min before the oral administration of rotenone. The rotenone-induced loss of TH-positive neurons in the SNpc was significantly inhibited by the injection of UCP0054278 at both 1 and 3 mg/kg (Fig. 6: A and B).

In the striatum of rotenone-treated mice, TH immunoreactivity was significantly decreased (Fig. 6A). However, TH immunoreactivity was markedly restored by UCP0054278 (Fig. 6A). Semi-quantitative analysis showed that the intensity of TH-immunoreactivity in the striatum was significantly increased by UCP0054278 (Fig. 6C).

Effect of peripheral administration of UCP0054278 on intracellular α-synuclein immunoreactivity in the SNpc of rotenone-treated mice

A previous study showed that the oral administration of rotenone at 30 mg/kg for 56 days produced some TH-positive neurons, which induced a high level of cytoplasmic α-synuclein immunoreactivity, in the SNpc (39). To examine the effect of UCP0054278 on intracellular α-synuclein immunoreactivity in the SNpc, we performed a confocal microscopic analysis. While TH-positive neurons were clearly detected in the SNpc of vehicle-treated mice, α-synuclein immunoreactivity was not detected in these TH-positive neurons (Fig. 7A). Although TH-positive neurons were obviously decreased by rotenone (Fig. 7A), α-synuclein immunoreactivity was detected in some surviving TH-positive neurons in the SNpc of rotenone-treated mice (Fig. 7A). The number of α-synuclein and TH double-positive cells was significantly increased in the SNpc of rotenone-lesioned mice (Fig. 7B). Interestingly, α-synuclein immunoreactivity was significantly decreased in the surviving TH-positive neurons in UCP0054278-treated rotenone mice (Figs. 7: A and B). In addition, the number of α-synuclein and TH double-positive cells was significantly decreased by treatment with UCP0054278 (Fig. 7B).

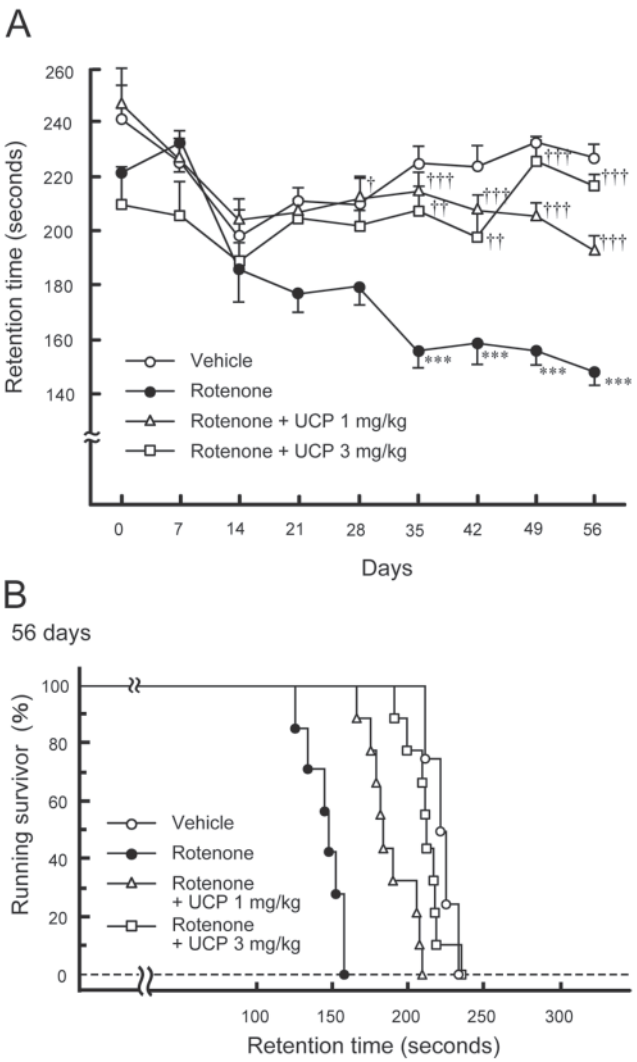

Fig. 5. Suppression of rotenone-induced behavioral dysfunction by UCP0054278. Rotenone (suspended in 0.5% CMC) was orally administered to C57BL/6 mice at a dose of 30 mg/kg per day for 56 days. In addition, we injected mice with vehicle (1% DMSO) or UCP0054278 at 1 or 3 mg/kg, i.p. once a day for 56 days, 30 min before the oral administration of rotenone. A: The rota-rod test was performed every week. The speed of the rotating rod was accelerated in a stepwise manner (2 r.p.m, steps at intervals of 30 s). Mice that had received oral rotenone showed significant motor dysfunction. This rotenone-induced dysfunction was significantly restored by UCP0054278 at 1 or 3 mg/kg. Significance: $^{***}P < 0.001$ vs. vehicle; $^{\dagger}P < 0.05$, $^{\dagger\dagger}P < 0.01$, $^{\dagger\dagger\dagger}P < 0.001$ vs. rotenone alone. B: Time-dependent changes in the percentage (%) of mice remaining on the rotating rod at 56 days. Mice that had received oral rotenone showed significantly greater motor dysfunction than those that had received vehicle at 56 days ($P = 0.0039$ by the log-rank test). Rotenone-induced motor dysfunction was significantly restored by UCP0054278 at both 1 mg/kg ($P < 0.001$) and 3 mg/kg ($P < 0.001$).

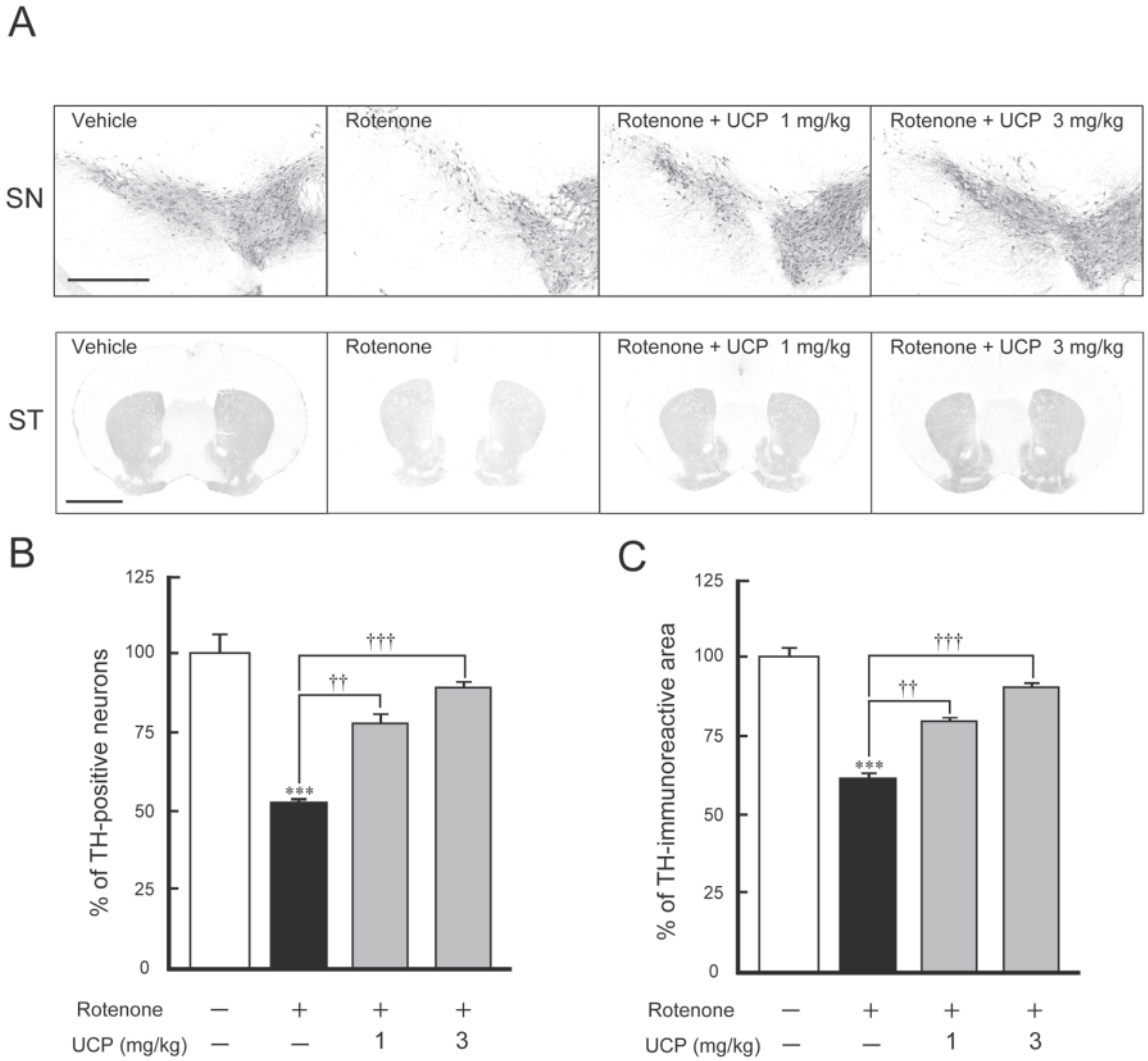

Fig. 6. Suppression of rotenone-induced dopaminergic neurodegeneration by UCP0054278. Rotenone (suspended in 0.5% CMC) was orally administered to C57BL/6 mice at a dose of 30 mg/kg per day for 56 days. In addition, we injected mice with vehicle (1% DMSO) or UCP0054278 at 1 or 3 mg/kg, i.p. once a day for 56 days, 30 min before the oral administration of rotenone. After the behavior test, rats were sacrificed and their brains were quickly removed for immunohistochemical analysis. A: Representative photomicrographs of immunoreactivity for TH in the substantia nigra and striatum. Scale bar: 500 μm. B: Stereological analysis of TH-positive neurons in the substantia nigra. C: Semi-quantitative analysis of TH-immunoreactive areas (mm^2) of the striatum. Each value is the mean ± S.E.M. (n = 6 in each group). Significance: ***$P < 0.001$ vs. vehicle; $^{\dagger\dagger}P < 0.01$, $^{\dagger\dagger\dagger}P < 0.001$ vs. rotenone alone.

Effect of UCP0054278 in in vitro neural cell cultures

SH-SY5Y cells are frequently used as a human dopaminergic neural model (42). We previously established DJ-1–knockdown SH-SY5Y cells, in which the expression of endogenous DJ-1 was suppressed by approximately 76%, as an in vitro model of PD (31). Therefore, in the present study we focus on the effect of UCP0054278 on 6-OHDA– or rotenone-mediated cell death in normal and DJ-1–knockdown SH-SY5Y cells.

In normal human SH-SY5Y cells, 6-OHDA caused cell death after 24 h in a concentration-dependent manner (Fig. 8A). This cell death was significantly inhibited by simultaneous treatment with UCP0054278 in a concentration-dependent manner. In DJ-1–knockdown SH-SY5Y cells, massive 6-OHDA–induced cell death occurred (Fig. 8B). Interestingly, UCP0054278 did not protect against 6-OHDA–induced cell death in DJ-1–knockdown cells. Similarly, in normal human SH-SY5Y cells, rotenone caused cell death after 48 h in a concentration-dependent manner (Fig. 8C). This cell death was significantly inhibited by simultaneous treatment with UCP0054278 in a concentration-dependent manner. In

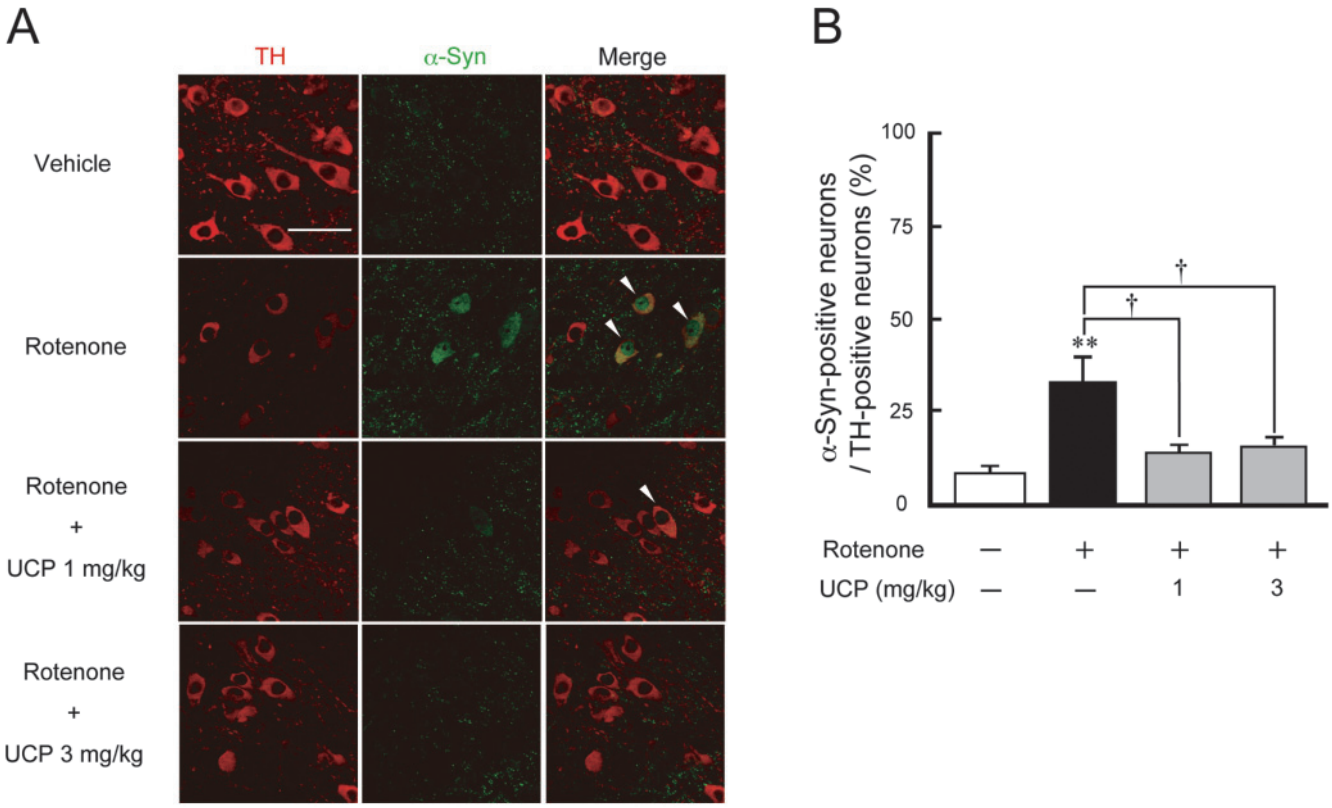

Fig. 7. Intracellular expression of α-synuclein in the substantia nigra. A: Nigral slices from mice treated with vehicle or rotenone at 30 mg/kg in the absence or presence of UCP0054278 at 1 or 3 mg/kg were co-incubated with antibodies to TH (red) and α-synuclein (green) and then analyzed by laser scanning confocal microscopy. Scale bar, 50 μm. B: Semi-quantitative analysis of TH- and α-synuclein-positive cells in the substantia nigra. The analysis of immunopositive cells was performed in the middle of the SNpc. Each value is the mean ± S.E.M. based on the number of immunopositive cells (each group, n = 6). Significance: $^{**}P < 0.01$ vs. vehicle and $^{\dagger}P < 0.05$ vs. rotenone alone.

DJ-1–knockdown cells, however, UCP0054278 did not protect against rotenone-induced cell death (Fig. 8D).

In normal SH-SY5Y cells, incubation with 50 μM 6-OHDA for 1 h induced marked intracellular ROS production (Fig. 9: A and B), while only slight fluorescence was induced by 25 μM 6-OHDA (Fig. 9: C and D). In DJ-1–knockdown cells, even 25 μM 6-OHDA induced significant fluorescence after 1 h (Fig. 9: C and D). On the other hand, simultaneous treatment with 10 μM UCP0054278 significantly inhibited ROS production, which had been induced by 50 μM 6-OHDA, in normal SH-SY5Y cells (Fig. 9: A and B). Unfortunately, in DJ-1–knockdown cells, this DJ-1 compound lost its inhibitory effect on ROS production induced by 25 μM 6-OHDA (Fig. 9: C and D). On the other hand, incubation with 100 nM rotenone for 1 h induced marked intracellular ROS production in both normal and DJ-1–knockdown SH-SY5Y cells (Fig. 9E). Similar to the effect of UCP0054278 on 6-OHDA–induced ROS production, simultaneous treatment with 10 μM UCP0054278 significantly inhibited rotenone-induced ROS production in normal SH-SY5Y cells, but not DJ-1–knockdown cells (Fig. 9: E and F).

Discussion

To understand the pathophysiology of PD and to develop therapies to improve the management of symptoms, it is important to have relevant disease models of PD, in which new pharmacological agents and treatment strategies can be assessed before clinical trials are initiated. For relevance to human PD, an ideal PD model should have the following characteristics: easily detectable Parkinsonian motor deficits, selective and gradual loss of DA neurons that develops with age, and production of Lewy-body–like cytoplasmic inclusions. Unfortunately, the life span of rodents is much shorter than that of humans, and they are limited with regard to their use as models for age-dependent disorders including PD, although age-dependency in rodents can be overcome by

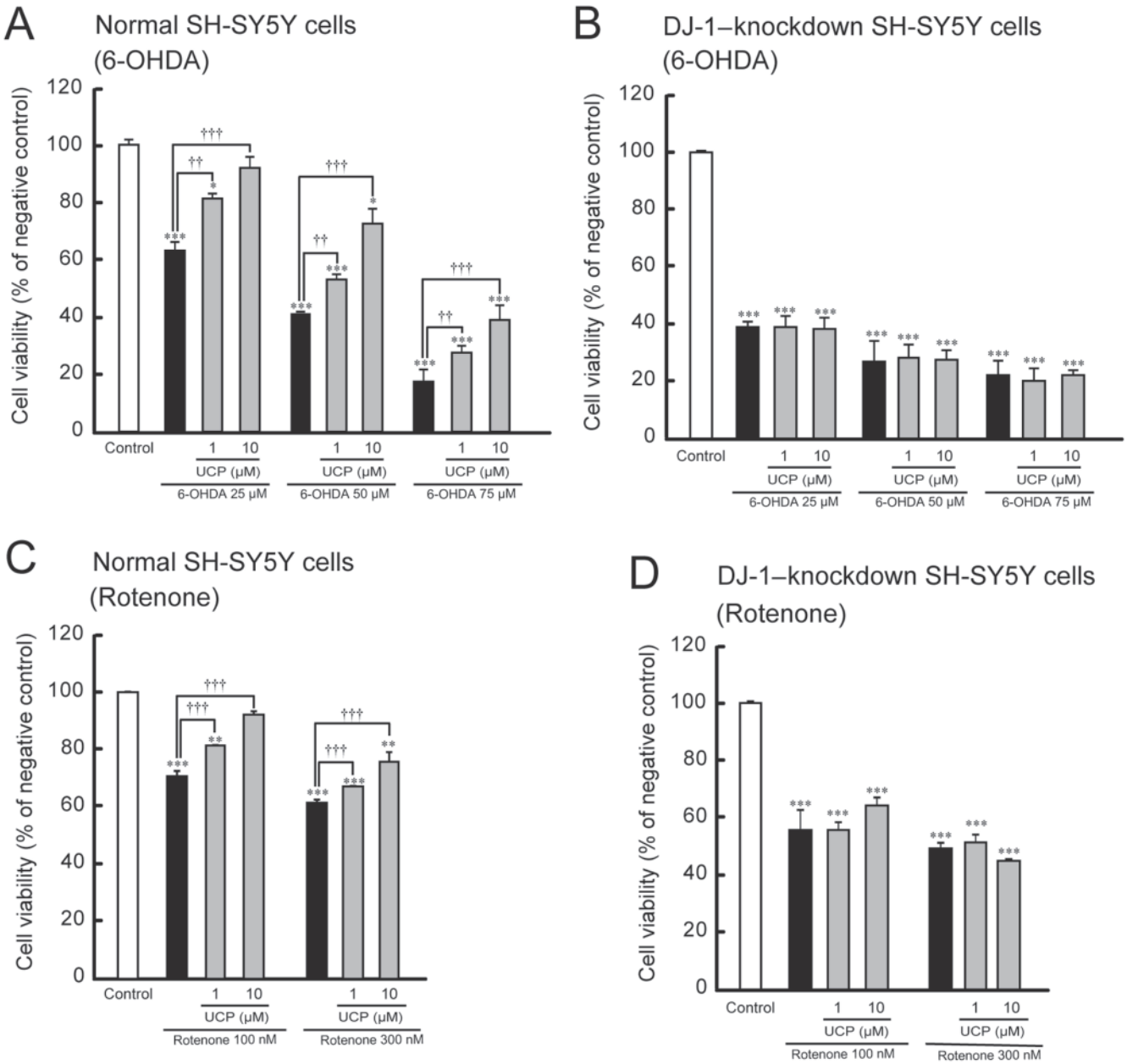

Fig. 8. Effect of simultaneous treatment with UCP0054278 on 6-OHDA– or rotenone-induced oxidative stress in human SH-SY5Y cells (A, C: normal) and DJ-1–knockdown cells (B, D). A, B: MTT assay for cell survival at 24 h after treatment with 6-OHDA (25, 50, 75 μM) in the absence or presence of UCP0054278 (at 1, 10 μM). C, D: MTT assay for cell survival at 48 h after treatment with rotenone (100, 300 nM) in the absence or presence of UCP0054278 (at 1, 10 μM). Each value is the mean ± S.E.M. of three determinations, based on the untreated culture as 100 % (control: open column). Significance: $^{*}P < 0.05$, $^{**}P < 0.01$, $^{***}P < 0.001$ vs. treatment with control; $^{\dagger\dagger}P < 0.01$, $^{\dagger\dagger\dagger}P < 0.001$ vs. treatment with 6-OHDA or rotenone alone.

the use of neurotoxins (2). At present, although the available model of PD with neurotoxins is imperfect, there have been advances in molecular medicine using a combination of these models. In the present study, therefore, we used 6-OHDA–microinjected rats and rotenone-treated mice as acute and chronic animal models of PD, respectively. We can compensate for most of the disadvantages of these models by using two models, and thus we examined the effect of the peripheral administration of UCP0054278 on 6-OHDA– or rotenone-induced dopaminergic cell death in vivo.

In the present study, either pre-treatment or post-treatment with UCP0054278 tended to improve 6-OHDA–induced behavioral dysfunctions and dopa-

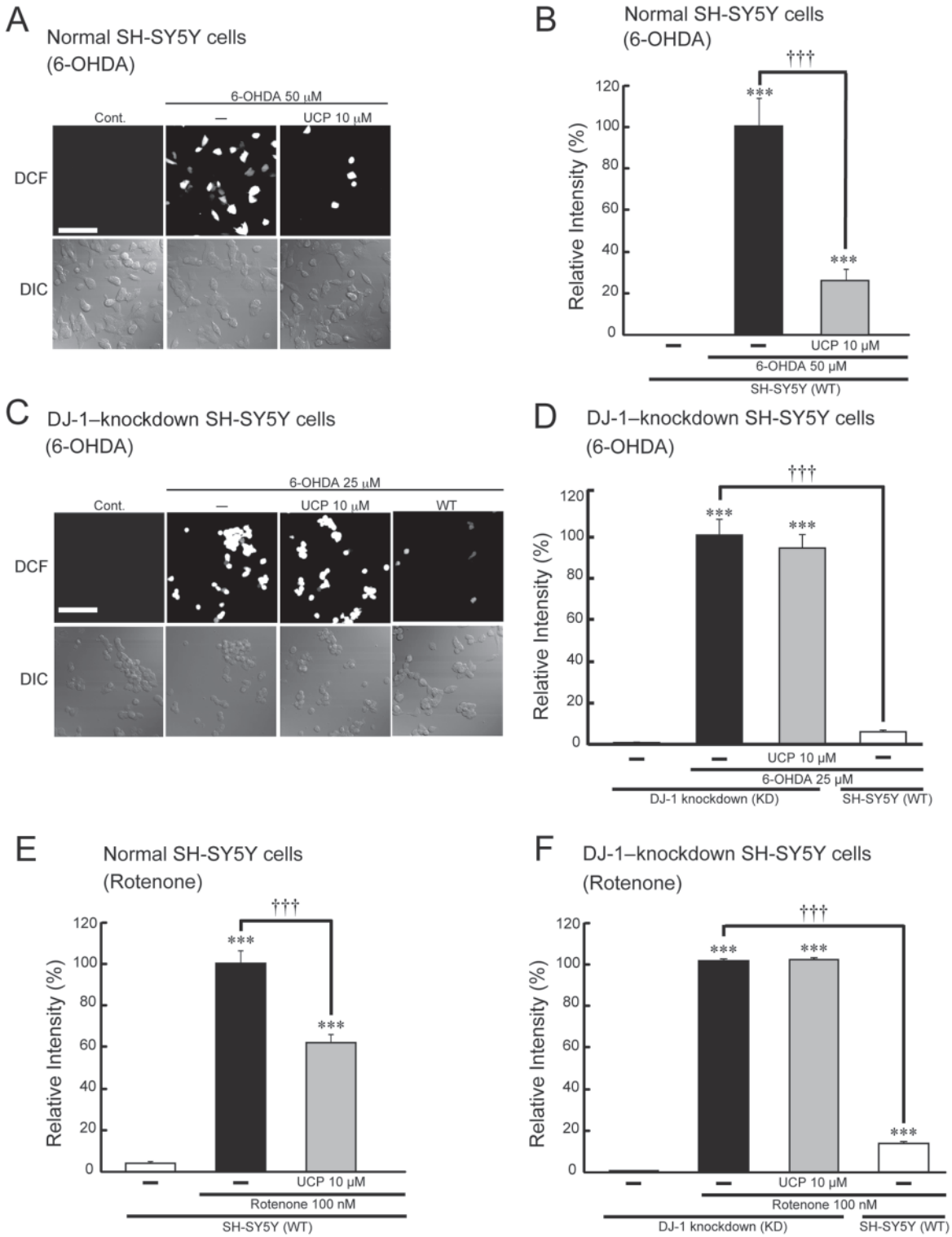

Fig. 9. Effect of UCP0054278 on 6-OHDA– or rotenone-induced ROS production. A – D: Normal and DJ-1–knockdown SH-SY5Y cells were treated with 50 μM (A, B) or 25 μM (C, D) 6-OHDA in the presence of vehicle (0.01% DMSO) or 10 μM UCP0054278 for 2.5 h. E, F: Normal and DJ-1–knockdown SH-SY5Y cells were treated with 100 nM rotenone in the presence of vehicle (0.01% DMSO) or 10 μM UCP0054278 for 24 h. Subsequently, CM-H_2DCFDA was added, and the fluorescence intensity of oxidized DCF was then visualized and measured by a confocal microscope. Cellular images were obtained by difference interference contrast (DIC). Data are the mean ± S.E.M. of three determinations, based on the intensity in cells treated with 6-OHDA or rotenone alone as 100%. Significance: ***$P < 0.001$ vs. vehicle and $^{\dagger\dagger\dagger}P < 0.001$ vs. 6-OHDA or rotenone alone. Scale bar: 50 μm.

minergic deficits, although these differences were not significant. On the other hand, pre- and post-treatment with UCP0054278 significantly ameliorated the behavioral impairment and prevented the dopaminergic neural cell death. In the rat experiment of the present study, we selected only one dose (1 mg/kg). Although the concentration dependence of UCP0054278 is unclear in the rat experiment, pre- and post-treatment with UCP0054278 may have shown synergistic neuroprotective effects. In further support of this supposition, in the in vitro experiment of the present study, 6-OHDA– or rotenone-induced cell death was significantly inhibited by treatment with UCP0054278 in a concentration-dependent manner. Furthermore, in the mouse experiment of the present study, rotenone-induced behavioral dysfunctions and dopaminergic deficits were significantly and concentration-dependently inhibited by treatment with UCP0054278.

Protein oxidation reflects the trapping of oxygen atoms (Os) in amino acid residues, that is, methionine and cysteine, are oxidized to Met-SO (1O) and Cys-SO_3H (3Os), respectively; and rodent and human DJ-1 protein has four methionine and three cysteine residues (43). On the other hand, oxidation at C106 is necessary for DJ-1 to exert an antioxidant response; and massive oxidation may cause a loss-of-function of DJ-1 (18, 43). By *in silico* virtual screening, we identified UCP0054278 as a DJ-1 modulator, which can bind to the SO_2H-oxidized C106 region. Direct binding between UCP0054278 and recombinant wild-type DJ-1 protein (but not C106S-mutated DJ-1, bovine serum albumin, or glutathione-S-transferase) was detected by a biosensor chip in a quartz crystal microbalance system (32), suggesting that UCP0054278 binding is relatively specific to wild-type DJ-1 protein and its binding site may be the C106 region. We previously showed that UCP0054278 itself could not directly scavenge $^{\bullet}OH$ based on an electron spin resonance (ESR) analysis (34). In addition to cytoplasmic, mitochondrial, and nuclear DJ-1, recent studies have reported that DJ-1 protein was detected in extracellular spaces, such as plasma and cerebrospinal fluids (44, 45), suggesting that DJ-1 protein may function in both intracellular and extracellular spaces. Therefore, we consider that UCP0054278 that has passed through the BBB binds to endogenous DJ-1 protein, and this DJ-1 / UCP0054278 complex has neuroprotective effects against ROS-mediated dopaminergic neurodegeneration.

In the present study, simultaneous treatment with UCP0054278 reduced ROS production and cell death induced by 50 μM 6-OHDA in normal SH-SY5Y cells. In DJ-1–knockdown cells, 6-OHDA at an even lower concentration (25 μM) significantly induced ROS production and cell death. However, DJ-1–knockdown caused the loss of UCP0054278-induced inhibitory effects toward ROS production and cell death. Similar results were also seen in rotenone-induced ROS production and cell death. DJ-1 has eliminating activity of ROS via the auto-oxidative mechanism (43). UCP0054278 itself can not directly scavenge $^{\bullet}OH$ (34). These results indicate that endogenous DJ-1 protein is necessary for the antioxidant and neuroprotective effects induced by UCP0054278. Since UCP0054278 binds to the SO_2H-oxidized C106 region in wild-type DJ-1 protein, it is possible that UCP0054278 stabilizes active DJ-1 with SO_2H-oxidized C106 and/or inhibits peroxidation to inactive DJ-1 with SO_3H-oxidized C106. Therefore, the UCP0054278 / DJ-1 complex may sustain eliminating activity of ROS via the auto-oxidative mechanism.

In the present study, we used two neurotoxins, 6-OHDA and rotenone. These neurotoxins inhibit mitochondrial complex I, resulting in the production of ROS. DJ-1 plays a role in maintenance of mitochondrial complex I activity (46 – 48). A previous study showed that the UCP0054278 / DJ-1 complex prevented loss of mitochondrial complex I activity after 6-OHDA intoxication and that even without 6-OHDA intoxication, the UCP0054278 / DJ-1 complex stimulated mitochondrial complex I activity (32), suggesting that the UCP0054278 / DJ-1 complex may eliminate ROS via the maintenance of mitochondrial complex I activity.

In addition, DJ-1 induces indirect antioxidant episodes, which are mediated through the stabilizing nuclear factor erythroid 2–related factor (Nrf2) by preventing association with the Kelch-like erythroid cell-derived protein with cap‘n’collar homology (ECH)-associated protein-1 (Keap1), which results in the activation of antioxidant transcriptional responses such as the induction and enhanced expression of NAD(P)H quinine oxidoreductase-1 (NQO1), heme oxygenase-1, superoxide dismutase-1, thioredoxin, and so on (49). On the other hand, recent studies have reported that DJ-1 inhibits several apoptotic pathways such as pyrimidine tract–binding protein-associated splicing factor (PSF) / 54-kDa nuclear RNA-binding protein (p54nrb) pathway (25) and/or apoptosis signal regulating kinase 1 (ASK1) / homeodomain-interacting protein kinase (HIPK1) / death-domain–associated protein (Daxx) pathway (25, 50). Moreover, DJ-1 may act to maintain mitochondrial function during oxidative stress, and thereby alter mitochondrial dynamics and autophagy indirectly (51, 52). Based on these observations, we consider that the UCP0054278 / DJ-1 complex may maintain and enhance DJ-1–induced anti-oxidative and anti-apoptotic activation, and these responses may synergistically act to prevent both ROS production and neural cell death. Therefore, UCP0054278 interacted with endogenous DJ-1 to inhibit 6-OHDA– or rotenone-

induced ROS production and neural cell death in both the in vivo and in vitro models of PD. These findings raise the possibility that UCP0054278 may be a new type of dopaminergic neuroprotective drug for the treatment of PD.

In conclusion, this is the first report to show that the peripheral administration of UCP0054278 has a neuroprotective effect in in vivo PD models. UCP0054278 may bind to the SO_2H-oxidized C106 region in endogenous DJ-1 protein and then maintain DJ-1–induced antioxidative and anti-apoptotic responses. The present results suggest that DJ-1 stimulatory modulators, such as UCP0054278, may be useful for neuroprotective treatment in cytoprotective therapy for various oxidative stress–mediated disorders.

Acknowledgments

This study was supported in part by Frontier Research Programs from the Ministry of Education, Culture, Sports, Science, and Technology (MEXT) and by the Program for Promotion of Fundamental Studies in Health Sciences of the National Institute of Biomedical Innovation (NIBIO) in Japan.

References

1 Dunnett SB, Björklund A. Prospects for new restorative and neuroprotective treatments in Parkinson's disease. Nature. 1999; 399 Suppl:A32–A39.
2 Shimohama S, Sawada H, Kitamura Y, Taniguchi T. Disease model: Parkinson's disease. Trends Mol Med. 2003;9:360–365.
3 Parker WD Jr, Boyson SJ, Parks JK. Abnormalities of the electron transport chain in idiopathic Parkinson's disease. Ann Neurol. 1989;26:719–723.
4 Schapira AH, Cooper JM, Dexter D, Jenner P, Clark JB, Marsden CD. Mitochondrial complex I deficiency in Parkinson's disease. Lancet. 1989;3:1269.
5 Mann VM, Cooper JM, Krige D, Daniel SE, Schapira AH, Marsden CD. Brain, skeletal muscle and platelet homogenate mitochondrial function in Parkinson's disease. Brain. 1992; 115:333–342.
6 Mizuno Y, Yoshino H, Ikebe S, Hattori N, Kobayashi T, Shimoda-Matsubayashi S, et al. Mitochondrial dysfunction in Parkinson's disease. Ann Neurol. 1998;44:S99–S109.
7 Polymeropoulos MH, Lavedan C, Leroy E, Ide SE, Dehejia A, Dutra A, et al. Mutation in the alpha-synuclein gene identified in families with Parkinson's disease. Science. 1997;276:2045–2047.
8 Kitada T, Asakawa S, Hattori N, Matsumine H, Yamamura Y, Minoshima S, et al. Mutations in the parkin gene cause autosomal recessive juvenile parkinsonism. Nature. 1998;392:605–608.
9 Leroy E, Boyer R, Auburger G, Leube B, Ulm G, Mezey E, et al. The ubiquitin pathway in Parkinson's disease. Nature. 1998; 395:451–452.
10 Bonifati V, Rizzu P, van Baren MJ, Schaap O, Breedveld GJ, Krieger E, et al. Mutations in the DJ-1 gene associated with autosomal recessive early-onset parkinsonism. Science. 2003;299: 256–259.
11 Valente EM, Abou-Sleiman PM, Caputo V, Muqit MM, Harvey K, Gispert S, et al. Hereditary early-onset Parkinson's disease caused by mutations in PINK1. Science. 2004;304:1158–1160.
12 Paisan-Ruiz C, Jain S, Evans EW, Gilks WP, Simon J, van der Brug M, et al. Cloning of the gene containing mutations that cause PARK8-linked Parkinson's disease. Neuron. 2004;44: 595–600.
13 Zimprich A, Biskup S, Leitner P, Lichtner P, Farrer M, Lincoln S, et al. Mutations in LRRK2 cause autosomal-dominant parkinsonism with pleomorphic pathology. Neuron. 2004;44:601–607.
14 Nagakubo D, Taira T, Kitaura H, Ikeda M, Tamai K, Iguchi-Ariga SMM, et al. DJ-1, a novel oncogene which transforms mouse NIH3T3 cells in cooperation with ras. Biochem Biophys Res Commum. 1997;231:509–513.
15 Takahashi K, Taira T, Niki T, Seino C, Iguchi-Ariga SMM, Ariga H. DJ-1 positively regulates the androgen receptor by impairing the binding of PIASx alpha to the receptor. J Biol Chem. 2001; 276:37556–37563.
16 Niki T, Takahashi-Niki K, Taira T, Iguchi-Ariga SMM, Ariga H. DJBP: a novel DJ-1-binding protein, negatively regulates the androgen receptor by recruiting histone deacetylase complex, and DJ-1 antagonizes this inhibition by abrogation of this complex. Mol Cancer Res. 2003;1:247–261.
17 Yokota T, Sugawara K, Ito K, Takahashi R, Ariga H, Mizusawa H. Down-regulation of DJ-1 enhances cell death by oxidative stress, ER stress, and proteasome inhibition. Biochem Biophys Res Commun. 2003;312:1342–1348.
18 Taira T, Saito Y, Niki T, Iguchi-Ariga SMM, Takahashi K, Ariga H. DJ-1 has a role in antioxidative stress to prevent cell death. EMBO Rep. 2005;5:213–218.
19 Canet-Aviles RM, Wilson MA, Miller DW, Ahmad R, McLendon C, Bandyopadhyay S, et al. The Parkinson's disease protein DJ-1 is neuroprotective due to cysteine-sulfinic acid-driven mitochondrial localization. Proc Natl Acad Sci U S A. 2004;101:9103–9108.
20 Shendelman S, Jonason A, Martinat C, Leete T, Abeliovich A. DJ-1 is a redox-dependent molecular chaperone that inhibits alpha-synuclein aggregate formation. PLoS Biol. 2004;2:e362.
21 Martinat C, Shendelman S, Jonason A, Leete T, Beal MF, Yang L, et al. Sensitivity to oxidative stress in DJ-1-deficient dopamine neurons: an ES-derived cell model of primary parkinsonism. PLoS Biol. 2004;2:e327.
22 Shinbo Y, Taira T, Niki T, Iguchi-Ariga SMM, Ariga H. DJ-1 restores p53 transcription activity inhibited by Topors/p53BP3. Int J Oncol. 2005;26:641–648.
23 Shinbo Y, Niki T, Taira T, Ooe H, Takahashi-Niki K, Maita C, et al. Proper SUMO-1 conjugation is essential to DJ-1 to exert its full activities. Cell Death Diff. 2006;13:96–108.
24 Sekito A, Koide-Yoshida S, Niki T, Taira T, Iguchi-Ariga SMM, Ariga H. DJ-1 interacts with HIPK1 and affects H_2O_2-induced cell death. Free Radic Res. 2006;40:155–165.
25 Xu J, Zhong N, Wang H, Elias JE, Kim CY, Woldman I, et al. The Parkinson's disease-associated DJ-1 protein is a transcriptional co-activator that protects against neuronal apoptosis. Hum Mol Genet. 2005;14:1231–1241.
26 Fan J, Ren H, Ji N, Fei E, Zhou T, Jiang P, et al. DJ-1 decreases bax expression through repressing p53 transcriptional activity. J Biol Chem. 2008;283:4022–4030.
27 Junn E, Jang WH, Zhao X, Jeong BS, Mouradian MM. Mito-

chondrial localization of DJ-1 leads to enhanced neuroprotection. J Neurosci Res. 2009;87:123–129.
28 Ishikawa S, Taira T, Niki T, Takahashi-Niki K, Maita C, Maita H, et al. Oxidative status of DJ-1-dependent activation of dopamine synthesis through interaction of tyrosine hydroxylase and 4-dihydroxy-L-phenylalamine (L-DOPA) decarboxylase with DJ-1. J Biol Chem. 2009;284:28832–28844.
29 Ishikawa S, Taira T, Niki T, Takahashi-Niki K, Ariga H, Iguchi-Ariga SM. Human DJ-1-specific transcriptional activation of tyrosine hydroxylase gene. J Biol Chem. 2010;285:39718–39731.
30 Inden M, Taira T, Kitamura Y, Yanagida T, Tsuchiya D, Takata K, et al. PARK7 DJ-1 protects against degeneration of nigral dopaminergic neurons in Parkinson's disease rat model. Neurobiol Dis. 2006;24:144–158.
31 Yanagisawa D, Kitamura Y, Inden M, Takata T, Taniguchi T, Morikawa S, et al. DJ-1 protects against neurodegeneration caused by focal cerebral ischemia and reperfusion in rats. J Cereb Blood Flow Metab. 2008;28:563–578.
32 Miyazaki S, Yanagida T, Nunome K, Ishikawa S, Inden M, Kitamura Y, et al. DJ-1-binding compounds prevent oxidative stress-induced cell death and movement defect in Parkinson's disease model rats. J Neurochem. 2008;105:2418–2434.
33 Yamane K, Kitamura Y, Yanagida T, Takata K, Yanagisawa D, Taniguchi T, et al. Oxidative neurodegeneration is prevented by UCP0045037, an allosteric modulator for the reduced form of DJ-1, a wild-type of familial Parkinson's disease-linked PARK7. Int J Mol Sci. 2009;10:4789–4804.
34 Yanagida T, Kitamura Y, Yamane K, Takahashi K, Takata K, Yanagisawa D, et al. Protection against oxidative stress-induced neurodegeneration by a modulator for DJ-1, the wild-type of familial Parkinson's disease-linked PARK7. J Pharmacol Sci. 2009;109:463–468.
35 Yanagida T, Tsushima J, Kitamura Y, Yanagisawa D, Takata K, Shibaike T, et al. Oxidative stress induction of DJ-1 protein in reactive astrocytes scavenges free radicals and reduces cell injury. Oxid Med Cell Longev. 2009;2:36–42.
36 Kinumi T, Kimata J, Taira T, Ariga H, Niki E. Cysteine-106 of DJ-1 is the most sensitive cysteine residue to hydrogen peroxide-mediated oxidation in vivo in human umbilical vein endothelial cells. Biochem Biophys Res Commun. 2004;317:722–728.
37 Ungerstedt U. Postsynaptic supersensitivity after 6-hydroxydopamine induced degeneration of the nigro-striatal dopamine system. Acta Physiol Scand. 1971;Suppl 367:69–93.
38 Inden M, Kitamura Y, Takeuchi H, Yanagida T, Takata K, Kobayashi Y, et al. Neurodegeneration of mouse nigrostriatal dopaminergic system induced by repeated oral administration of rotenone is prevented by 4-phenylbutyrate, a chemical chaperone. J Neurochem. 2007;101:1491–1504.
39 Inden M, Kitamura Y, Abe M, Tamaki A, Takata K, Taniguchi T. Parkinsonian rotenone mouse model: reevaluation of long-term administration of rotenone in C57BL/6 mice. Biol Pharm Bull. 2011;34:92–96.
40 Hanisch UK, Kettenmann H. Microglia: active sensor and versatile effector cells in the normal and pathologic brain. Nat Neurosci. 2007;10:1387–1394.
41 Kitamura Y, Nomura Y. Stress proteins and glial functions: possible therapeutic targets for disorders. Pharmacol Ther. 2003; 97:35–53.
42 Kitamura Y, Kosaka T, Kakimura J, Matsuoka Y, Kohno Y, Nomura Y, et al. Protective effects of antiparkinsonian drugs talipexole and pramipexole against 1-methyl-4-phenylpyridinium-induced apoptotic death in human neuroblastoma SH-SY5Y cells. Mol Pharmacol. 1998;54:1046–1054.
43 Zhou W, Zhu M, Wilson MA, Petsko GA, Fink AL. The oxidation state of DJ-1 regulates its chaperone activity toward alpha-synuclein. J Mol Biol. 2006;356:1036–1048.
44 Allard L, Burkhard PR, Lescuyer P, Burgess JA, Walter N, Hochstrasser DF, et al. PARK7 and nucleoside diphosphate kinase A as plasma markers for the early diagnosis of stroke. Clin Chem. 2005;51:2043–2051.
45 Waragai M, Wei J, Fujita M, Nakai M, Ho G, Masliah E, et al. Increased level of DJ-1 in the cerebrospinal fluids of sporadic Parkinson's disease. Biochem Biophys Res Commun. 2006; 345:967–972.
46 Hayashi T, Ishimori C, Takahashi-Niki K, Taira T, Kim YC, Maita H, et al. DJ-1 binds to mitochondrial complex I and maintains its activity. Biochem Biophys Res Commun. 2009;390: 667–672.
47 Blackinton J, Lakshminarasimhan M, Thomas KJ, Ahmad R, Greggio E, Raza AS, et al. Formation of a stabilized cysteine sulfinic acid is critical for the mitochondrial function of the parkinsonism protein DJ-1. J Biol Chem. 2009;284:6476–6485.
48 Guzman JN, Sanchez-Padilla J, Wokosin D, Kondapalli J, Ilijic E, Schumacker PT, et al. Oxidant stress evoked by pacemaking in dopaminergic neurons is attenuated by DJ-1. Nature. 2010; 468:696–700.
49 Clements CM, McNally RS, Conti BJ, Mak TW, Ting JP. DJ-1, a cancer-and Parkinson's disease-associated protein, stabilizes the antioxidant transcriptional master regulator Nrf2. Proc Natl Acad Sci U S A. 2006;103:15091–15096.
50 Junn E, Taniguchi H, Jeong BS, Zhao X, Ichijo H, Mouradian MM. Interaction of DJ-1 with Daxx inhibits apoptosis signal-regulating kinase 1 activity and cell death. Proc Natl Acad Sci U S A. 2005;102:9691–9696.
51 Thomas KJ, McCoy MK, Blackinton J, Beilina A, van der Brug M, Sandebring A, et al. DJ-1 acts in parallel to the PINK1/parkin pathway to control mitochondrial function and autophagy. Hum Mol Genet. 2011;20:40–50.
52 McCoy MK, Cookson MR. DJ-1 regulation of mitochondrial function and autophagy through oxidative stress. Autophagy. 2011;7:531–532.